International Journal of Mechanical, Industrial and Aerospace Sciences
ISSN: 2517-9950
Vol:9, No:10, 2015

Polymer Aerostatic Thrust Bearing Under Circular Support for High Static Stiffness

S. W. Lo, C.-H. Yu

Abstract**—**A new design of aerostatic thrust bearing is proposed for high static stiffness. The bearing body, which is mead of polymer covered with metallic membrane, is held by a circular ring. Such a support helps form a concave air gap to grasp the air pressure. The polymer body, which can be made rapidly by either injection or molding is able to provide extra damping under dynamic loading. The smooth membrane not only serves as the bearing surface but also protects the polymer body. The restrictor is a capillary inside a silicone tube. It can passively compensate the variation of load by expanding the capillary diameter for more air flux. In the present example, the stiffness soars from 15.85 N/μm of typical bearing to 349.85 N/μm at bearing elevation 9.5 μm; meanwhile the load capacity also enhances from 346.86 N to 704.18 N.

Keywords**—**Aerostatic, bearing, polymer, static stiffness.

I. Introduction

AEROSTATIC bearings have been employed widely in coordinate measurement and ultra-precision machining due to their high accuracy and near-frictionless running characteristics [1]. However, they are suffering from the relatively low stiffness and load capacity as compared to roller and hydrostatic bearings due to the compressibility of air medium. Both passive and active approaches have been carried out to overcome these weaknesses. Compared to the active compensations, the passive ones possess the advantages of relatively low cost since no complicated sensors, actuators, amplifiers, data processing units, etc. are needed. The structures and therefore the construction procedures are much simpler.

The passive methods include the use of restrictor like capillary or orifice next to the nozzle, modifying the air flow [2], using porous material [3] or similar material like woven wire cloth [4]. All aim to improve the pressure distribution for better stiffness, reduce the vibration, or eliminate the resonance owing to the stimulating force.

Recently, [5] proposed a new concept of using capillary inside a silicone tube as the restrictor and a polymer bulk covered with metallic membrane as the bearing body, as shown in Fig. 1. The viscoelastic nature of polymers adds particular benefits to the bearing design in several aspects. The silicone restrictor shows subtle response to the change in the recess pressure since the impedance of the capillary is inversely proportional to the capillary radius to the fourth power. Therefore a tiny expansion of the capillary may lead to considerable passive compensation of the air flux. On the other hand, the bulk polymer allows the bearing surface to form a converging profile automatically by the air pressure to increase the load capability. Furthermore, the viscous energy dissipation might provide additional damping to the bearing system if the bearing operates under dynamic external force to alleviate the tendency towards, say, pneumatic hammering. The 0.2 mm thick metal membrane, which is cut from any standard "ready-to-use" product, offers a smooth surface of stable quality. In addition to eliminate the irregular, wavy surface of polymer body, it provides an extra protection to melting down in case of solid contact between bearing and the fast-moving counterpart. His numerical study shown that compared to the load capacity 309 N and static stiffness 21 N/μm at film thickness (elevation) 10 μm for the conventional bearing of diameter 60 mm under supply pressure 0.5 MPa (5 bar), the optimal outputs for the new design are leveled up to 506 N and 102 N/μm, respectively.

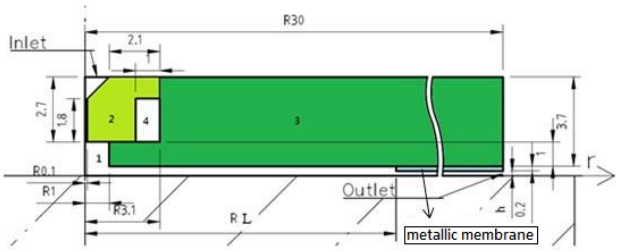

Fig. 1 Polymer body with metal membrane at bottom [5]; the bearing is supported on the tops of components 2 and 3

According to the inclusive literature reviews of Al-Bender [6], a converging (concave) bearing surface is able to level up the load capacity since the conicity of the air gap helps sustain the air pressure. The concave geometry is usually obtained by shaping the bearing into a circularly supported disk which can be bent by the pressurized air. In the present paper, we intend to propose a novel design which combines the polymer bearing body of Lu [5] with the idea of circular support to attain better static stiffness. Taking the bearing with diameter of 60 mm as an example, the adequate radius where the polymer disk is supported will be investigated. The optimal dimensions, material properties of polymer body as well as the metallic cover will be suggested by means of Taguchi method.

S. W. Lo is with the Department of Mechanical Engineering, National Yunlin University of Science and Technology, Douliu City, 640 Yunlin, Taiwan (Phone: +886-5-5342601 ext. 4140; Fax: +886-5-5312062; e-mail: losw@ yuntech.edu.tw).

C.-H. Yu is with the Department of Mechanical Engineering, National Yunlin University of Science and Technology, Douliu City, 640 Yunlin, Taiwan (e-mail: m10111053@yuntech.edu.tw).

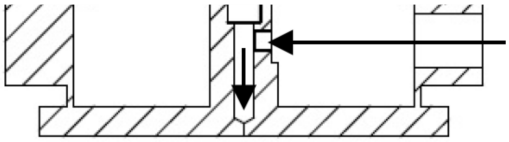

Fig. 2 Cross section of circular supported aluminum 6061 bearing, the details of nozzle and restrictor are not shown. Air pipe is inserted in the wall of the center column

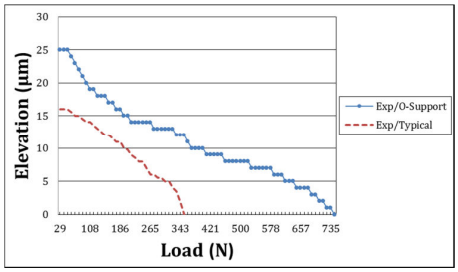

Fig. 3 Experimental elevations between typical and circular supported aluminum 6061 bearings both have identical restrictor and nozzle

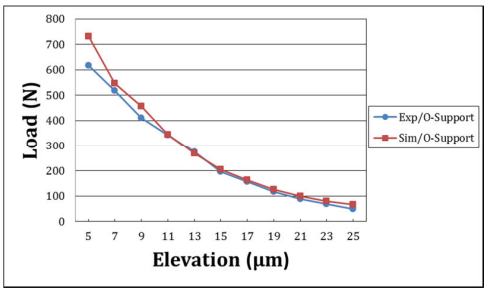

Fig. 4 Comparison between simulation (red) and experimental (blue) results

II. Validation of Numerical Simulation

The research will be conducted based on a series of numerical simulations utilizing the commercial code COMSOL. The first task is to verify the accuracy of the simulation. Therefore a typical aerostatic thrust bearing and a circularly supported one as shown in Fig. 1 are tested. Both bearings are made of aluminum alloy 6061 and possess 60 mm diameter of bearing surface, inlet hole of 2 mm diameter, 1.8 mm-long capillary of 0.2 mm diameter, following a pocket of 2 mm diameter and 1 mm depth. The 2.5 mm-thick disk is buttressed at the position of radius 25 mm. All the experiments are operated under supply air pressure 5 bar (0.5MPa) at room temperature about 20°C.

As for the simulation, the axisymmetric mode of numerical code is used to save the computational time. The modulus of steady, turbulent air at 293 K and the material properties of AL 6061 alloy: Young's modulus 76.6 GPa and Poisson ratio 0.33, are chosen. The influence of the mesh size on the numerical output is also investigated and the default normal one is found to be satisfactory. Details are depicted in Yu [7].

The elevations of the bearing with respect to its rest position for different external loads are shown in Fig. 3 and the comparison between experiment and simulation is given in Fig. 4. In Fig. 3 the circular supported one is marked as "O-support" and the results reflects that it really demonstrates superior load ability and stiffness. Fig. 4 validates that the computation is accurate enough; particular for elevation above 10 μm. Below this height the simulation generally shows greater load capacities than the measured ones. This might due to not only the neglect of the influences of the surface roughness, which anticipates decreasing the levitation effect, but also the slip between fluid and solid boundary. It might result from the resolution (2 μm) of the dial indicator as well, so that the measurement actually is an underestimation.

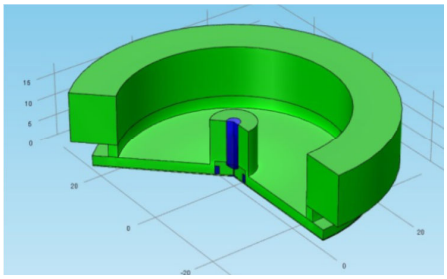

(a)

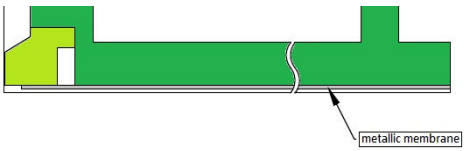

(b)

Fig. 5 (a) 3D complete illustration of the circular supported polymer bearing; the displacement of the top of the upper, larger support ring with respect to its rest position is defined as the elevation of the bearing, (b) Sectional illustration of the lower part of the circular supported polymer bearing

III. Simulation Procedures

In the following section, the calculation will extend to the case of circularly supported polymer disk which has a silicone restrictor and a bearing surface covered by metallic membrane, as shown in Figs. 5 (a) and (b). Different metals are used. The properties of the metals and the polymers in COMSOL are listed in Tables I and II, respectively. Some of them are default. Note that the Young's modulus of the PU chosen here is much greater than that used by Lu [5] due to the need of stronger disk for circular support.

The calculation procedures are as follows: firstly, the elevation of the top of the upper, bigger support ring in Fig. 5 (a) is assigned in the code. The elevation is defined as the displacement of the top of the bigger ring with respect to its rest position and is equal to the uniform film thickness (gap) between bearing and counter surface when the air is not fed. Then the air fills in the chamber with its pressure gradually enhanced to 0.5 MPa (5 bar) at the top of silicone tube and flows through the gap to the brink of the disk where the pressure drops to zero. The gap is no more uniform since the pressurized air will push the disk to bend. For each given

elevation the pressure in the gap is integrated to get the load capacity of the bearing. The stiffness for each film thickness is approximated by typical finite difference skill.

TABLE I
MECHANICAL PROPERTIES OF METALLIC MEMBRANES

Material	Symbol	Young's Modulus	Poisson ratio
Aluminum alloy (UNS A96061)	AL	76.59324 GPa	0.33
Copper alloy (UNS C11000)	CU	137 GPa	0.33
Midium carbon steel (UNS G10450)	G	221.7366 GPa	0.28
Stainless steel (UNS S30300)	SUS	212.6806 GPa	0.28

TABLE II
MECHANICAL PROPERTIES OF POLYMERS

Material	Young's modulus	Poisson ratio
Silicone	2.9 MPa	0.48
PU	17.25 GPa	0.40

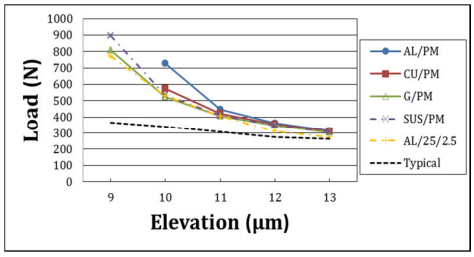

Fig. 6 Load vs. elevation for different structure and material combinations. AL/PM represents polymer body covered by aluminum alloy 6061, etc.; AL/25/2.5 denotes 2.5 mm-thick AL disk supported at radius 25 mm

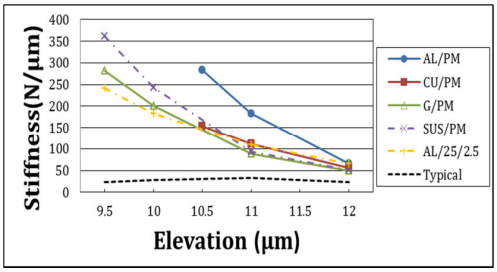

Fig. 7 Static stiffness vs. elevation for different structures and material combinations

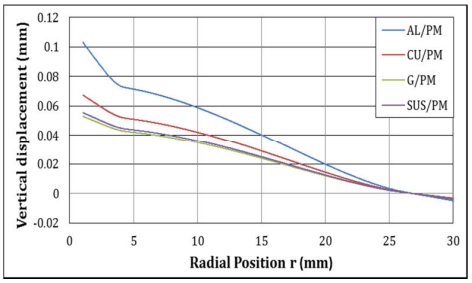

Fig. 8 Vertical displacement of the disk bearing surface, measured from the center to the brim of the disk at elevation 10 μm

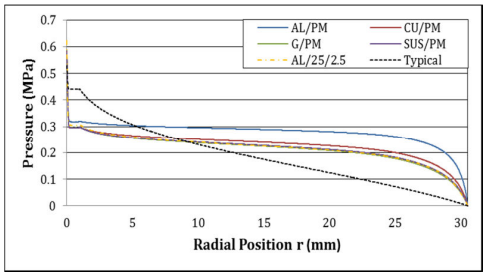

Fig. 9 Air pressure distribution along the bearing surface, measured from the center to the brim of the disk at elevation 10 μm

IV. RESULTS AND DISCUSSIONS

Fig. 6 depicts the load-elevation curves for various designs including the typical one and the flexible ones: the 2.5 mm-thick aluminum disk, and the polymer body covered with aluminum alloy 6061 (AL/PM), copper (CU/PM), medium carbon steel (G/PM) and stainless steel (SUS/PM), respectively; all flexible polymer disks have thickness of 2.5 mm and are supported at radius 25 mm. Figs. 6 and 7 show that the AL/PM bearing exhibits the best performance like load capacity and stiffness for load below 750 N. It can endure nearly 750N while sustains 10 μm of elevation. The static stiffness at elevation 10.5 μm is above 250 N/μm while the typical one can only provide about 30 N/μm. These superior abilities arise from the fact shown in Fig. 8 that the "softer" aluminum membrane displays greater deformation, therefore a converging bearing surface to maintain the pressure, exclusively near the disk brim. However, it is noteworthy that the excessive lift of the center part, say, the air pocket will cause a serious drop in inlet air pressure.

As the load grows beyond 750 N, the deformations of the aluminum membrane and the silicone tube are so severe that no numerical solution can be found. Only the "harder" membrane can offer the sufficient rigidity. At elevation 9 μm, the design using stainless steel executes better than that of pure metal AL/25/2.5. It can levitate 9 μm under nearly 900 N; its stiffness at 9.5 mm is over 350 N/μm.

V. DESIGNS FOR OPTIMAL STATIC STIFFNESS

In this section, the Taguchi method is adopted to find the optimal designs for stiffness at elevation 9.5 μm. Table III lists the factors: width, height, and the radius of the support ring and the three associated levels. Fig. 10 is the schematic illustration of the factors. The combination of these levels for the optimal static stiffness is found to be (A1, B3, C1), that is, a narrower and thicker ring of smaller radius. Various load-elevation curves are plotted in Fig. 11 and their calculated loads and stiffnesses are listed in Table IV. It can be seen that not only the stiffness but also the load capability improves a lot. The stiffness soars from 15.85 N/μm of typical bearing to 349.85 N/μm at elevation 9.5 μm; meanwhile the load capacity enhances from 346.86 N to 704.19 N.

TABLE III
FACTORS FOR TAGUCHI METHOD

Factor	Geometry	Level 1	Level 2	Level 3
A	Width of Ring	2.05mm	2.1mm	2.15mm
B	Height of Ring	2.8mm	3mm	3.2mm
C	Radius of Ring	24.5mm	25mm	25.5mm

TABLE IV
LOAD CAPACITY AND STATIC STIFFNESS FOR VARIOUS DESIGNS

Design	Load Capacity at Different Elevations			Stiffness at 9.5 μm
	9.25 μm	9.5 μm	9.75 μm	
Typical	349.34 N	346.86 N	341041 N	15.85 μm/N
Original	745.50 N	597.40 N	588.66 N	313.68 μm/N
Optimal	812.48 N	704.19 N	637.56 N	349.85 μm/N

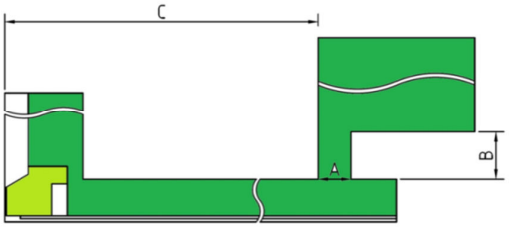

Fig. 10 Schematic illustration of factors: A=ring width; B= ring height; C= radius of ring

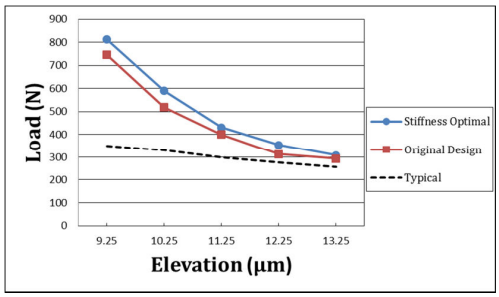

Fig. 11 Comparison between the case of optimal stiffness (A1, B3, C1) and others; Original marks the design SUS/PM in Fig. 7

ACKNOWLEDGMENT

The authors would like to thank the National Yunlin University of Science and Technology for the use of its facilities. The support from the National Science Council under grant NSC 102- 2221- E- 224- 014- MY3 is also gratefully acknowledged.

REFERENCES

[1] Y.-B. P. Kwan and J.B. Post, "A tolerancing procedure for inherently compensated, rectangular aerostatic thrust bearings," *Tribology International*, vol. 33, pp. 581-585, 2000.
[2] T. Aoyama, Y. Kakinuma, and Y. Kobayashi, "Numerical and experimental analysis for the small vibration of aerostatic guideways," *Annals of the CIRP- Manufacturing Tech.*, vol. 55 (1), pp. 419-422, 2006.
[3] S. Yoshimoto and K. Kohno, "Static and dynamic characteristics of aerostatic circular porous thrust bearings (effect of the shape of the air supply area)," *ASME Trans., J. Tribology*, vol. 123 (3), pp. 501-508, 2001.
[4] G. Belforte, T. Raparelli, V. Viktorov, and A. Trivella, "Metal woven wire cloth feeding system for gas bearings," *Tribology International*, vol. 42, pp. 600-608, 2009.
[5] S.-H. Lu, *Study on the static characteristics of aerostatic thrust bearing combining metallic and polymer components*, Master Thesis, National Yunlin University of Science and Technology, Taiwan, June, 2014.
[6] F. Al-Bender, "On the modelling of the dynamic characteristics of aerostatic bearing films: From stability analysis to active compensation," *Precision Engineering*, vol. 33, pp. 117-126, 2009.
[7] C.-H. Yu, *Influences of the geometrical and material parameters on the static characteristics of metallic and polymer aerostatic thrust bearings*, Master Thesis, National Yunlin University of Science and Technology, Taiwan, January, 2015.